nature materials

Article

https://doi.org/10.1038/s41563-023-01495-3

Combinatorial treatment rescues tumour-microenvironment-mediated attenuation of MALT1 inhibitors in B-cell lymphomas

In the format provided by the authors and unedited

Table of Content

Supplementary Discussion

CD40L attenuates MALT1 inhibitor response in canine

The utility of comparative oncology research to advance the understanding of cancer biology and novel therapeutic development is gaining broad recognition[1]. Canine lymphomas are the most common hematologic malignancy in dogs and are reported closely to resemble their human disease counterparts[2-4]. A subset had increased expression of NF-κB pathway genes, mirroring human ABC-DLBCLs[4]. Recent studies have identified molecular similarities, such as increased expression of NF-κB pathway genes, of canine DLBCLs to human DLBCL and have introduced pet dogs[1-4] as a representative large animal model of human DLBCL for mechanistic and therapeutic studies[1-4]. We sought to incorporate a canine DLBCL example into our Ly-TME organoid system to assess if our observations were consistent across species. Primary lymphoma samples were obtained from consented canine patients at Cornell University Hospital for Animals (CUHA) and placed directly into media with 1% penicillin/streptomycin solution after excision. Primary tumor samples were implanted s.c. into the left flank of eight to ten-week-old NOD.Cg-rkdcscid Il2rgtm1Wjl/SzJ (NSG) mice were originally purchased from Jackson Laboratories (Catalog # 005557) under 2.5% isoflurane anesthesia. Prior to implantation, tumor fragments were washed with sterile PBS and then minced into pieces fine enough to pass through an 18-gauge needle. Tumor pieces were separated into 2mm3 volumes and drawn into a 1ml syringe along with 200ul PBS. This was then injected subcutaneously into the left flank just in front of the hind limb. Tumors were allowed to grow to a volume of no greater than 2000mm3 before passaging into subsequent mice. The same procedure was used during each passage into new mice using tumor fragments obtained from the previous passage. Prior to encapsulation in organoids, tumors were then dissociated into single cells using a phosphate buffer containing collagenase A (25,000 U/ml), dispase II (12.5 U/ml), and DNAse (500 U/ml) and mechanical disruption through a 70 μm cell strainer. Organoids encapsulating PDXs were cultured in RPMI supplemented with 25% FBS, 2 mM L-glutamine, and penicillin G/streptomycin and grown at 37˚C in a humidified atmosphere of 5% CO_2. Canine antibodies included mouse anti-dog CD20 (clone 6C12, Invivogen, catalog dcd20-mab11) with AlexaFluor488-labeled goat anti-mouse IgG secondary (clone Poly4053, Biolegend or Life Technologies) and anti-MHC II (FITC, Clone YKIX334.2, eBioscience, catalog MCA1044GA).

Working with a canine DLBCL PDX specimen, we showed significantly reduced cell death in 3D than in 2D culture in the presence of CD40L stromal cells (**Supplementary Figure 5**). When treated with 2000 nM MI2, canine PDX cells displayed ~90% CD20+ cell viability relative to untreated cells when cultured with CD40L, compared to 5% viability relative to untreated cells in the absence of CD40L (**Extended Figure 3E**). Collectively, these results suggest that CD40L-mediated signaling from T cells can affect the efficacy of MALT1 inhibitors, especially under more physiological 3D conditions, and are conserved across species. Canine PDX cultures with CD40L support exhibited the same significant decrease and 60% killing in dual-treated cultures even with a low dose of idelalisib (**Extended Figure 9A**).

MI2 treatment did not kill MALT1^{hi}-expressing cells

To understand how Ly-TME might attenuate treatment response to MALT1 inhibition, we examined the effect of MI2 on MALT1 expression in ABC-DLBCL cells pooled from REDV- or GFOGER-functionalized hydrogels. GFOGER presentation led to a greater number of MALT1^{hi}-expressing cells (**Extended Figure 6A**). Exposure to MI2 reduced the proportion of MALT1^{hi}-

expressing cells in both GFOGER- and REDV-functionalized hydrogels in the absence of CD40L. In the presence of the CD40L signal, no such reduction in MALT1^{hi}-expressing cells was seen in GFOGER-functionalized hydrogels. MI2 treatment did not kill MALT1^{hi}-expressing cells in the presence of CD40L, suggesting that the CD40 pathway may be strongly amplifying cooperative signaling in ABC-DLBCLs. When tested across three human ABC-DLBCL PDXs, similar MALT1^{hi}-expressing cells and attenuated MI2 response were observed (**Extended Figure 6B**).

Ly-TME presentation increases cooperative signaling pathways

To determine the effect of GFOGER and CD40L presentation on cooperative signaling in ABC-DLBCLs, we performed RNA Sequencing on HBL1 cells cultured in hydrogel-based organoids presenting peptides REDV, GFOGER, or REDV with CD40L-stromal cells for 4 days. We performed differential expression (Log10FC>1, $p<0.05$) analysis (**Figure 4A**) and among the downregulated genes was the Tripartite Motif Containing 13 (*TRIM13)* which regulates AKT1 kinase activity and enhances ionizing radiation-induced p53/TP53 down-regulated genes included *EGR1* (Early Growth Response 1), which activates the expression of p53/TP53 and TGFB1 and thereby helps prevent tumor formation.

CD40L attenuates the response to BTK inhibitor ibrutinib

We evaluated whether the response to ibrutinib paralleled that of MALT1 inhibitors. The clinical efficacy displayed by ibrutinib in ABC-DLBCL has been challenged by the frequent emergence of resistant clones, causes of which are poorly understood. HBL1 cells cultured in GFOGER-functionalized hydrogels and treated with ibrutinib had a 6.4-fold increase in IC_{50} when compared to REDV-functionalized organoids (**Extended Figure 10A**). In contrast to GFOGER presentation, presence of CD40L-expressing stromal cells abrogated ibrutinib response even at high doses. GFOGER-presentation induced significantly higher levels of pBTK than REDV-presentation (**Extended Figure 10B**). Similarly, CD40L-presentation in REDV-functionalized gels significantly increased the expression of pBTK than gels without CD40L (**Extended Figure 10C, Supplementary Figure 12**). We next studied whether a combination of PI3K and BTK inhibition could overcome the CD40L-mediated dampened response. Both HBL1 and OCI-LY10 demonstrated a significant reduction in overall survival in REDV+CD40L presenting organoids when treated with combination therapeutics (**Extended Figure 10D**). OCI-LY3 cells that do not respond to PI3K or BTK inhibitors were not studied. Lastly, the combination of PI3K with BTK inhibitor could overcome the dual impact of CpG and CD40L (**Extended Figure 10E**). Collectively, these data indicate that in addition to MALT1-targeted therapy, BTK inhibitors are also impacted by Ly-TME, as elucidated by hydrogel-based organoids, and the therapeutic response of BTK inhibitors is significantly enhanced by targeted therapies that overcome cooperative Ly-TME signals.

Supplementary Figure 1

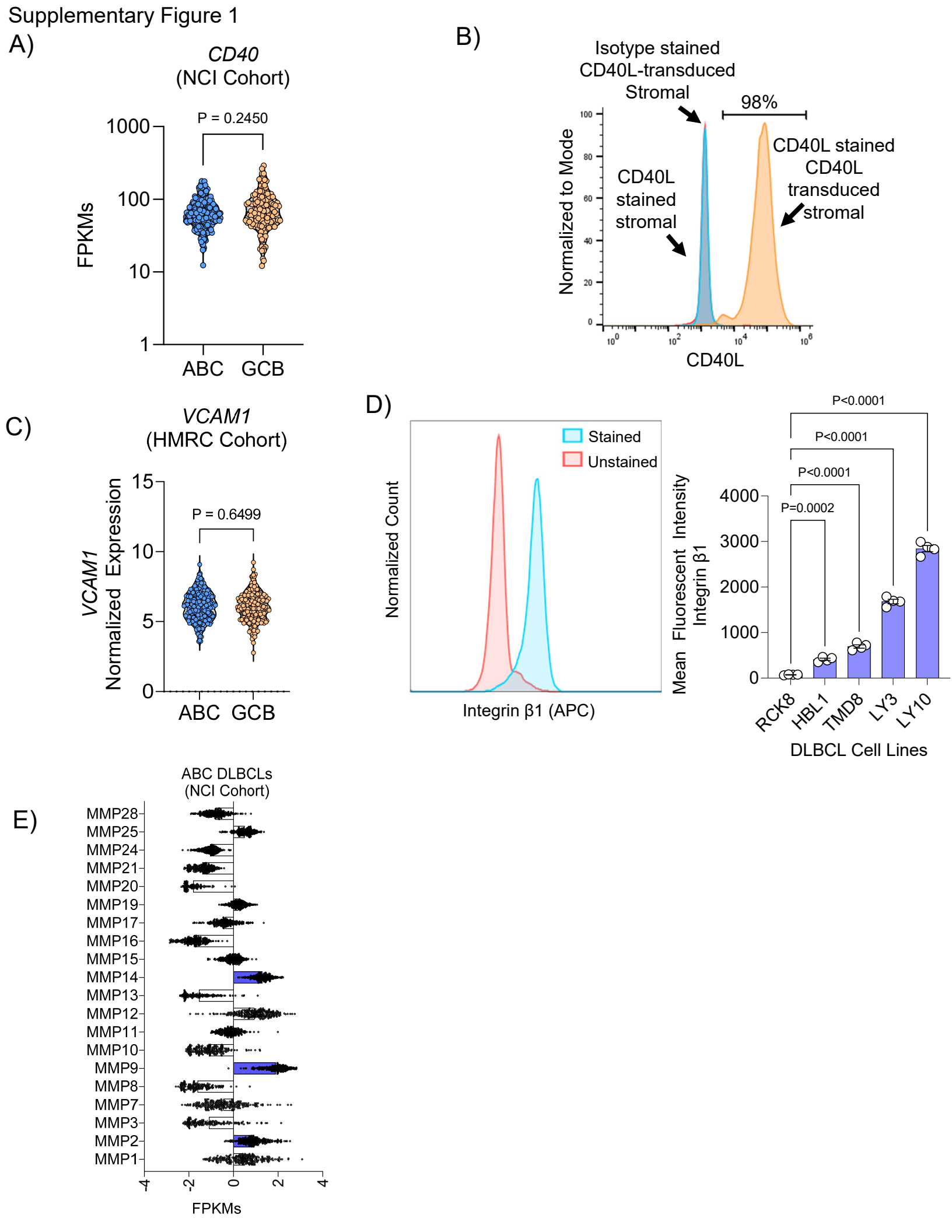

Supplementary Figure 1. Characterization of gene expression in the tumor microenvironment and cell protein expression.

A) Gene expression (FPKMs) of CD40 in ABC-DLBCL (n=243) and GCB-DLBCL (n=138) from the NCI cohort. Two-tailed unpaired t-test. B) Flow cytometry expression of CD40L in transduced 3T3 fibroblast cells. Controls include isotype-stained CD40L-transduced stromal cells and CD40L antibody-stained non-transduced stromal cells. C) Gene expression of VCAM1 in ABC-DLBCL (n=242) and GCB-DLBCL (n=264) patients from the HMRC cohort. Data were quantile normalized and $\log_2$ transformed. Two-tailed unpaired t-test. D) (Left) Representative flow histograms with unstained and stained cells on left. (Right) The expression level of integrin β1 on ABC-DLBCL cell lines by flow cytometry. One-way ANOVA with Tukey's multiple-comparison test (mean ± SEM, n=4, where each dot is a separate 2D culture). E) Gene expression (FPKMs) of MMPs in ABC-DLBCL (n=243) patients in the NCI cohort arranged in descending order. Blue color-coded MMPs are upregulated.

Supplementary Figure 2

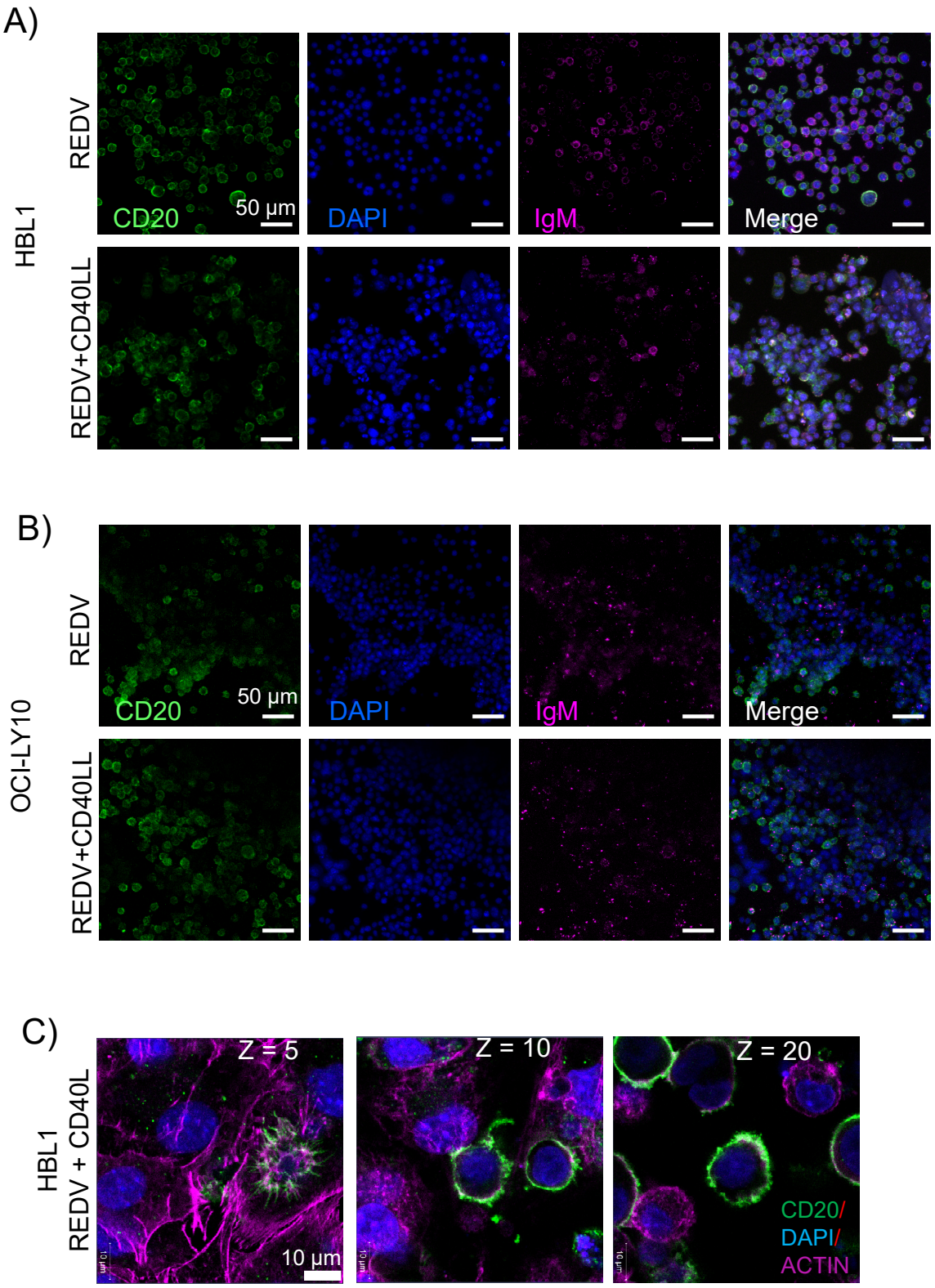

Supplementary Figure 2. CD40L-expressing stromal presentation clusters B cell lymphomas.

A-B) Confocal microscopy maximum intensity projection of z-stacks of PEG-4MAL hydrogel-based organoids with ABC-DLBCL cell lines HBL1 (A) and OCI-LY10 (B) with CD20 (Green), IgM BCR (magenta), and nucleus (DAPI, Blue). Cell lines were grown with or without CD40L-expressing stromal cells. Data representative of n=3 hydrogels. C) Confocal microscopy of z-stacks showing spread CD40L-expressing stromal cells (Actin, Purple) lacking CD20 expression (Green). Data representative of n=3 hydrogels.

Supplementary Figure 3

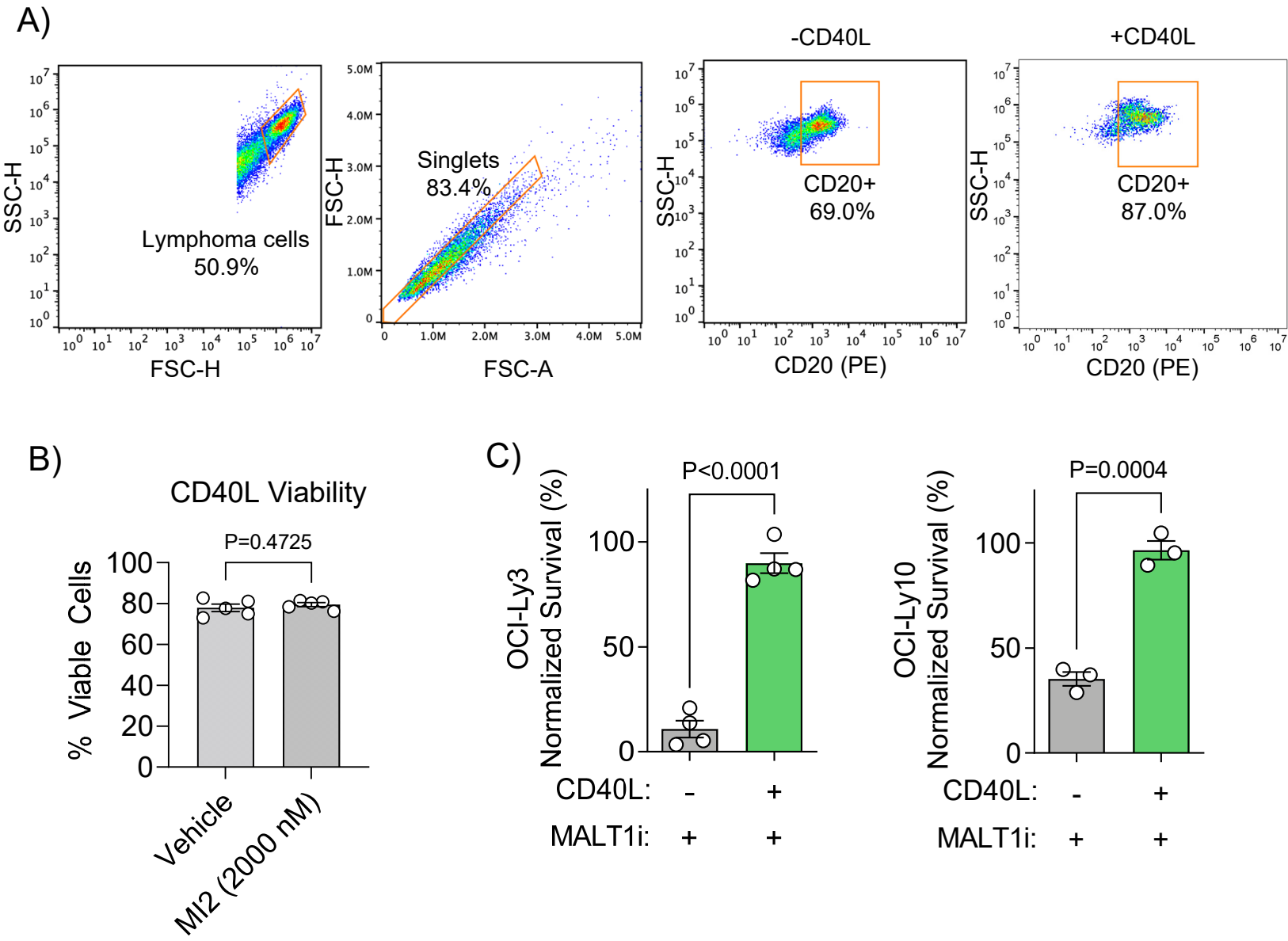

Supplementary Figure 3. Characterization of hydrogel-based organoid cultures.

A) Flow cytometry gating schematic for CD20+ DLBCL cells under ±CD40L conditions. B) Percent of viable CD40L expressing cells when exposed to vehicle or 2000 nM of MI2. . Two-tailed unpaired t-test. (mean ± SEM, n=5, each dot represents a hydrogel). C) Survival (normalized to vehicle-treated) of human ABC-DLBCL cell line OCI-Ly3 and OCI-LY10 cultured in organoids with and without CD40L after 96 hours of culture, consisting of 48 hours of 2000 nM MI2 treatment. Two-tailed unpaired t-test (mean ± SEM, n=4 for OCI-LY3 and n=3 for OCI-LY10, where each dot is a hydrogel-based organoid).

Supplementary Figure 4

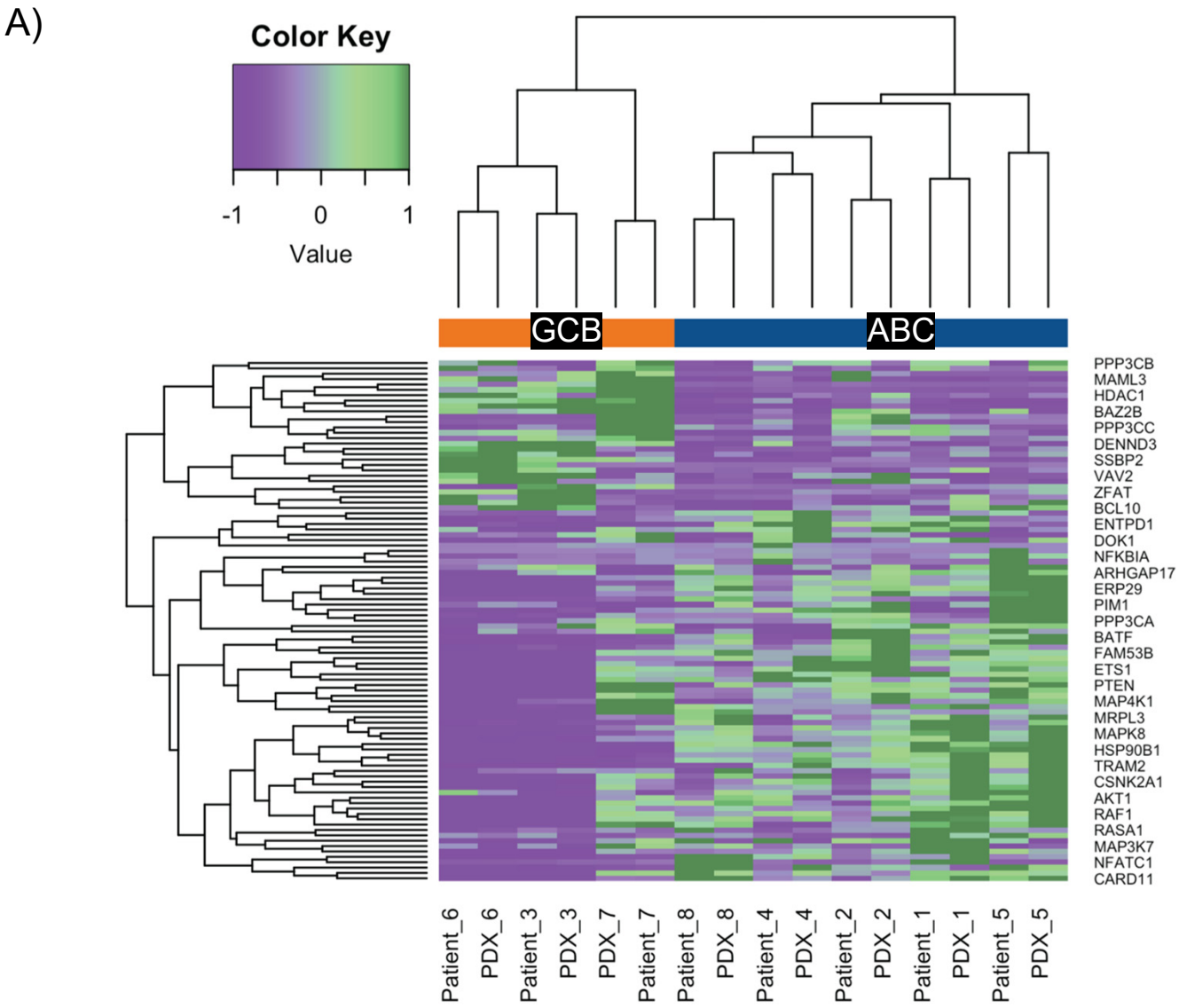

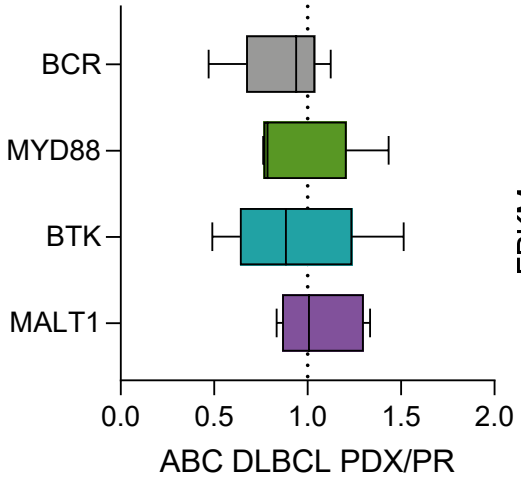

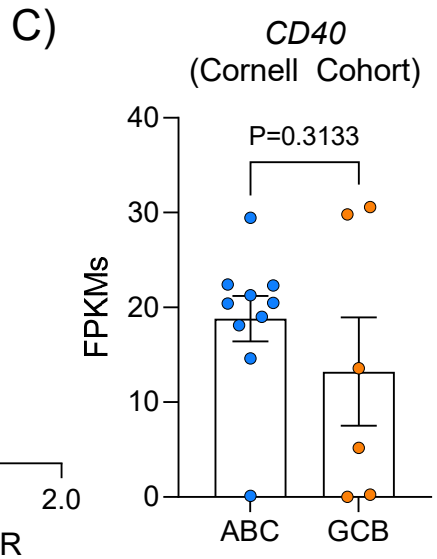

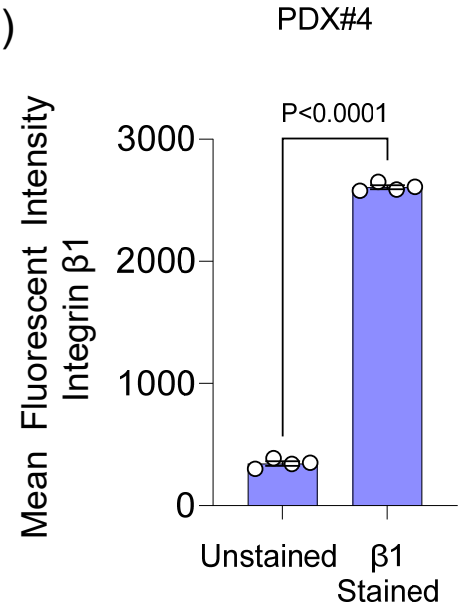

Supplementary Figure 4. Characterization of PDXs.

A) Heatmap of the BCR pathway and hallmark transcriptional genes for primary human DLBCLs samples (PR) and the resulting patient-derived xenografts (PDXs) from the Cornell cohort confirming assignment of samples into cell-of-origin (COO) groups. This cohort comprised of PDX and PR samples (n=10). B) The ratio of Cornell cohort ABC-DLBCL PDX expression with corresponding primary human DLBCLs samples (PR) (n=5) for characteristic BCR & TLR pathway genes, with a dotted line indicating PDX/PR=1. C) Gene expression (FPKMs) of CD40 in ABC (n=9) and GCB (n=6) DLBCL patients from NY cohort. Two-tailed unpaired t-test. mean ± SEM. D) Expression level of integrin β1 protein on ABC-DLBCL PDX by flow cytometry. Two-tailed unpaired t-test. (mean ± SEM, n=4, where each dot is a hydrogel-based organoid).

Supplementary Figure 5

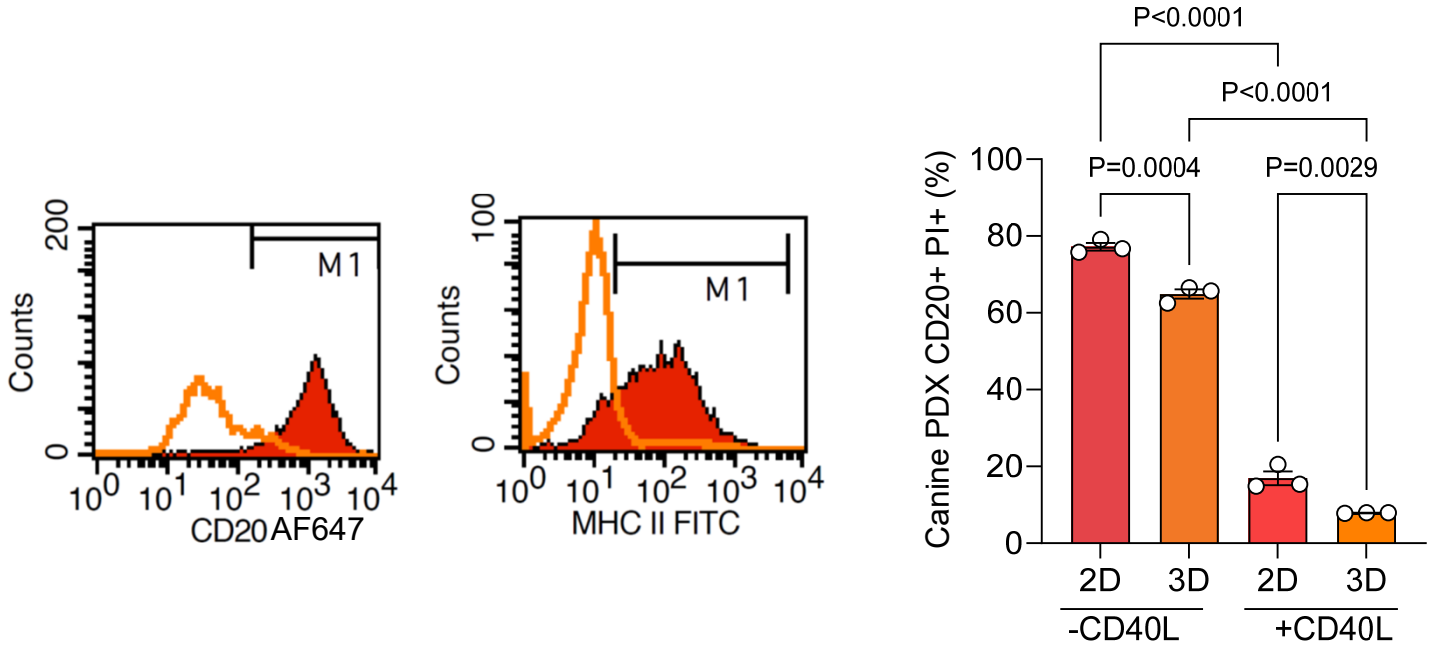

Supplementary Figure 5. Characterization of Canine PDXs and cultures.

Left: Representative CD20 and MHCII flow cytometry histograms with stained canine ABC DLBCL PDXs (red) Center & right: Percent of apoptotic canine ABC DLBCL PDX cells after 96-hour culture in either 2D or 3D organoids without or with CD40L (right). One-way ANOVA with Tukey's multiple-comparison test (mean ± SEM, n=3, where each dot is a hydrogel-based organoid).

Supplementary Figure 6

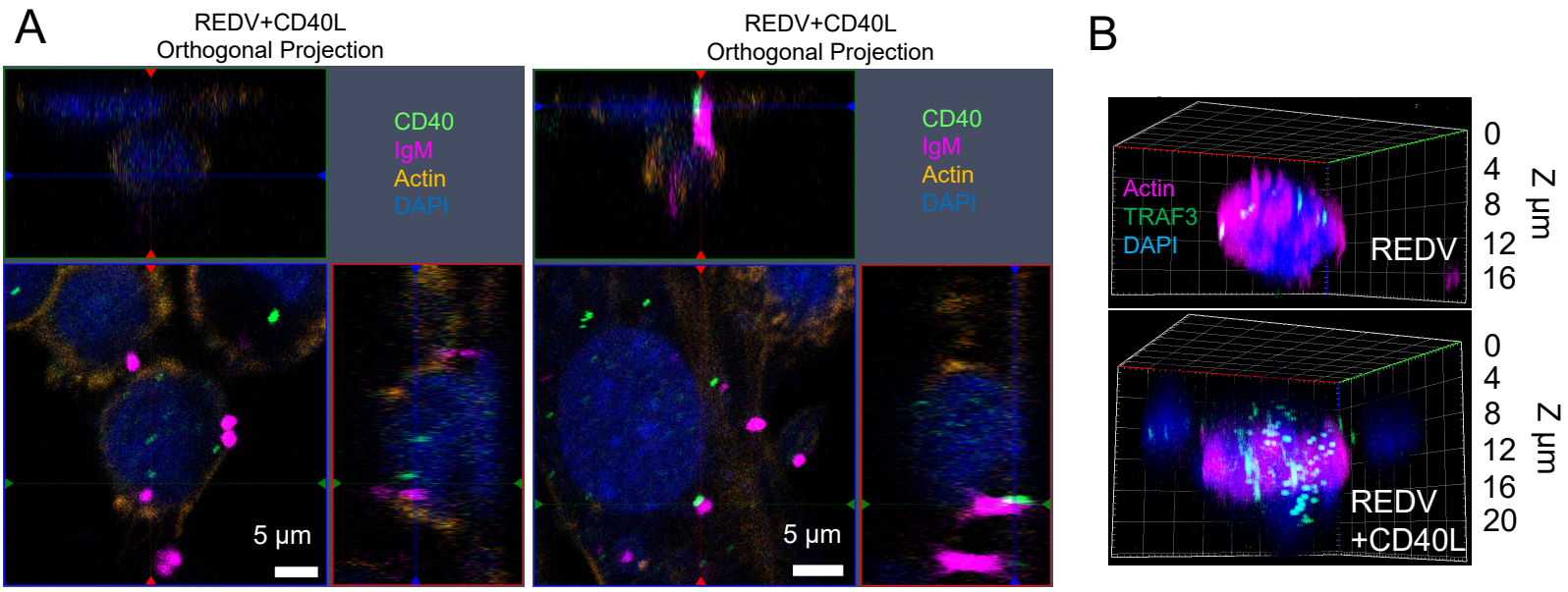

Supplementary Figure 6. Characterization of hydrogel-based organoids.

A) CD40 (green) spatial localization relative to BCR (magenta) puncta in HBL1 ABC-DLBCLs in the presence of CD40L-stromal cells. Orthogonal projections showing CD40L-stromal cells (spread, elongated) with DLBCL cells (spherical) in the hydrogel-based organoids. Data representative of n=3 organoids, 5 single cells per organoid. **B)** 3D projection of spatial expression of TRAF3 (green) in HBL1 ABC-DLBCLs grown in REDV-functionalized hydrogels in the presence or absence of CD40L-stromal cells, with TRAF3 (green), DAPI (blue) and actin (magenta). Data representative of n=3 organoids.

Supplementary Figure 7

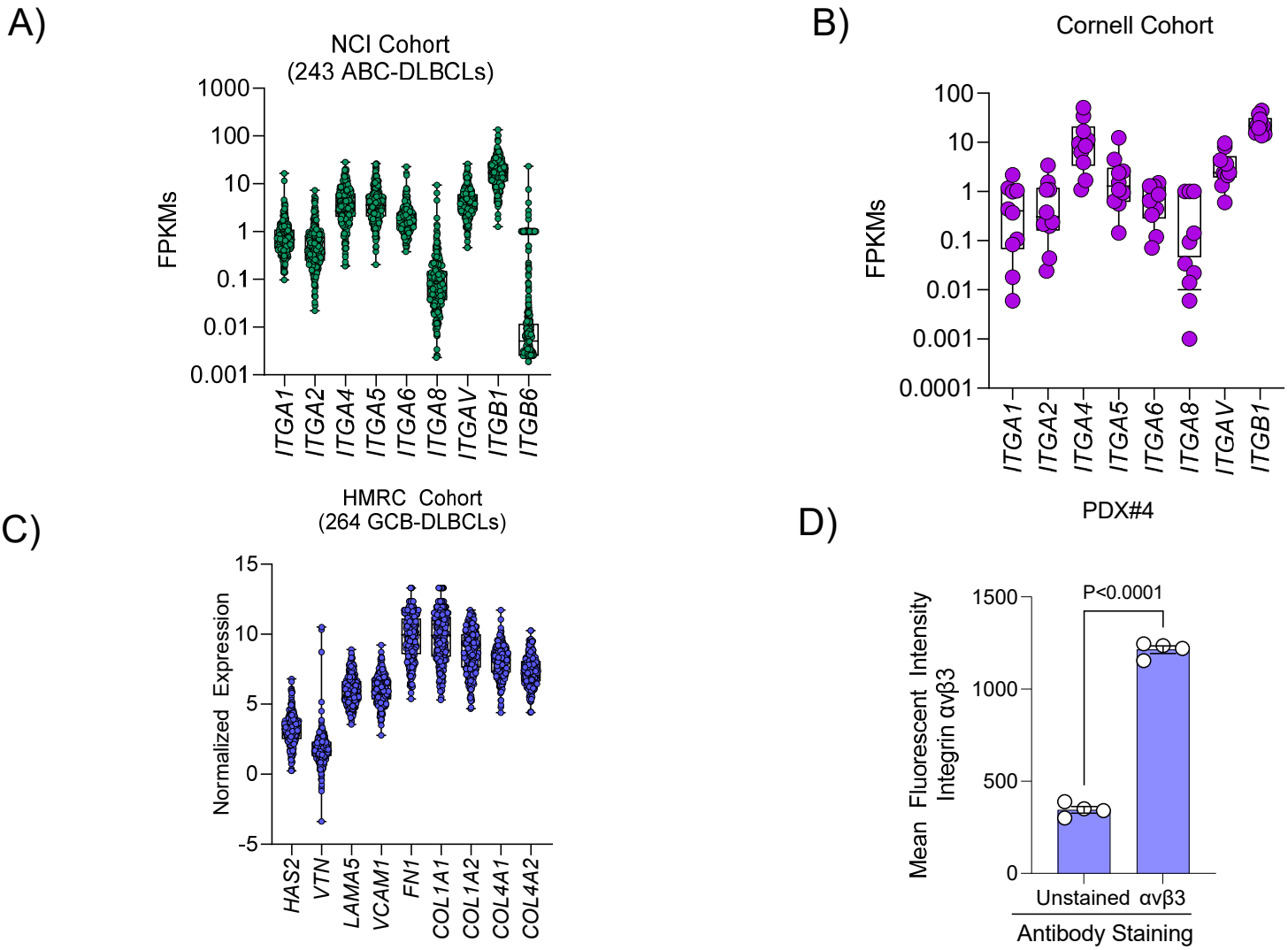

Supplementary Figure 7. Characterization of integrins and ECM in patient samples and PDXs.

A) Gene expression in fragments per kilobase million (FPKMs) of integrin α and β subunits in ABC-DLBCL samples (n=243) from the NCI cohort. B.) Gene expression (FPKMs) of integrinα subunits (left) and β subunits (right) for cohort ABC-DLBCL PDX and PR samples (n=10). C) Distribution of gene expression of ECM components in primary human GCB-DLBCLs (n = 264) samples from the HMRC cohort. D) Expression level of integrin $\alpha v\beta_3$ protein on ABC-DLBCL PDX by flow cytometry. Two-tailed unpaired t-test (mean ± SEM, n=4, where each dot is an explanted PDX from mice).

Supplementary Figure 8

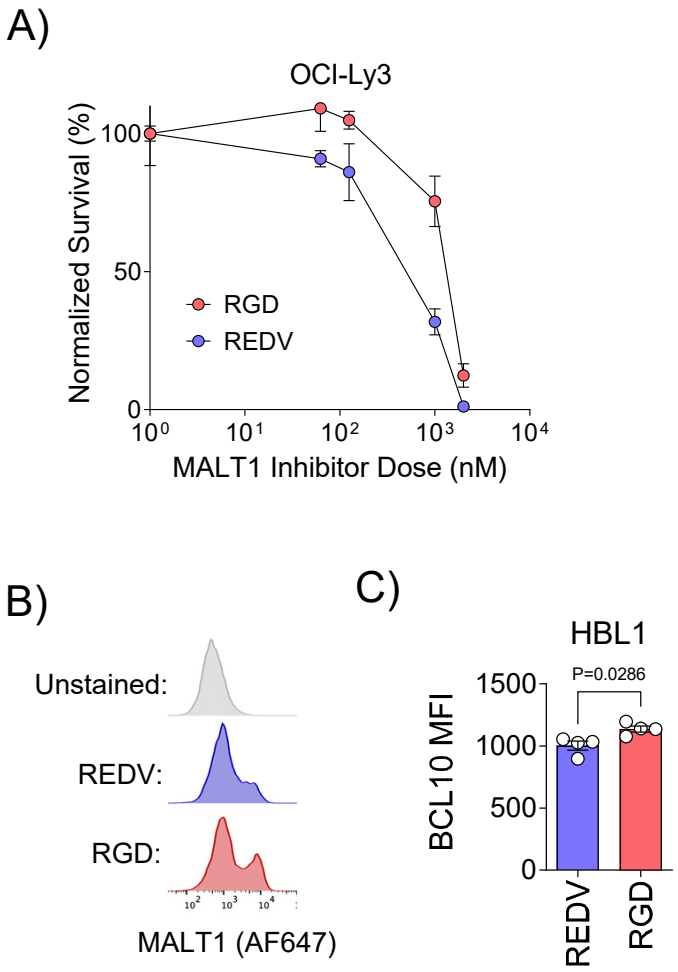

Supplementary Figure 8. Tumor cell survival and expression of MALT1 and BCL10 in organoids.

A) Survival (normalized to vehicle-treated) of ABC-DLBCL cell line Ly3 cultured in either RGD- (red) or REDV-functionalized hydrogels-based organoids (blue) after 48 hours of culture and subsequent 48 hours of treatment with increasing concentration of MALT1 inhibitor, MI2. Results indicate the mean ± SEM of 5 replicates. B-C) Representative flow histograms of MALT1 (B, for Fig. 1E) and median fluorescent intensity of BCL10 (C) measured via flow cytometry in HBL1 cells cultured in either RGD- (red) or REDV-functionalized hydrogels-based organoids (blue) for 96 hours. Two-tailed unpaired t-test (mean ± SEM, n=4, where each dot is a hydrogel-based organoid).

Supplementary Figure 9

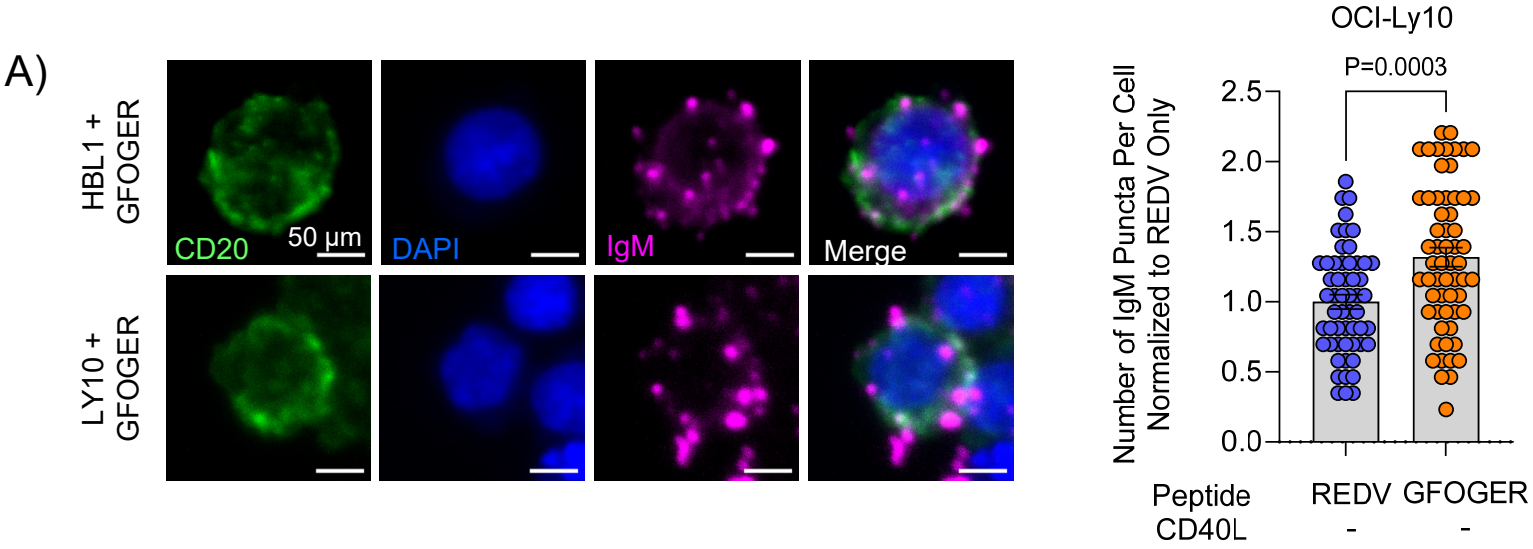

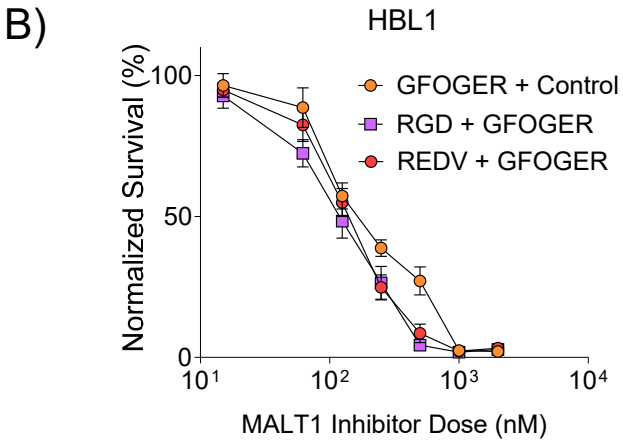

Supplementary Figure 9. BCR Puncta formation in organoids.

A) Left: BCR (magenta) puncta expression at the single-cell level on CD20 (green) expressing HBL1 (top) and OCI-Ly10 (bottom) in the presence of GFOGER peptides. Data representative of n = 5 organoids for each condition. Right: Number of BCR puncta per cell of OCI-LY10 ABC-DLBCL cells culture in ±CD40L-stromal cells. Two-tailed unpaired t-test (mean ± SEM, n=5 hydrogels with ~12 cells analyzed from each hydrogel).

B) Survival (normalized to vehicle-treated) of ABC-DLBCL cell line HBL1 cultured in GFOGER+control (orange), RGD+GFOGER (purple), or REDV+GFOGER (red) functionalized hydrogels-based organoids after 48 hours of culture and subsequent 48 hours of treatment with increasing concentration of MALT1 inhibitor, MI2. Results indicate the mean ± SEM of 5 hydrogel replicates.

Supplementary Figure 10

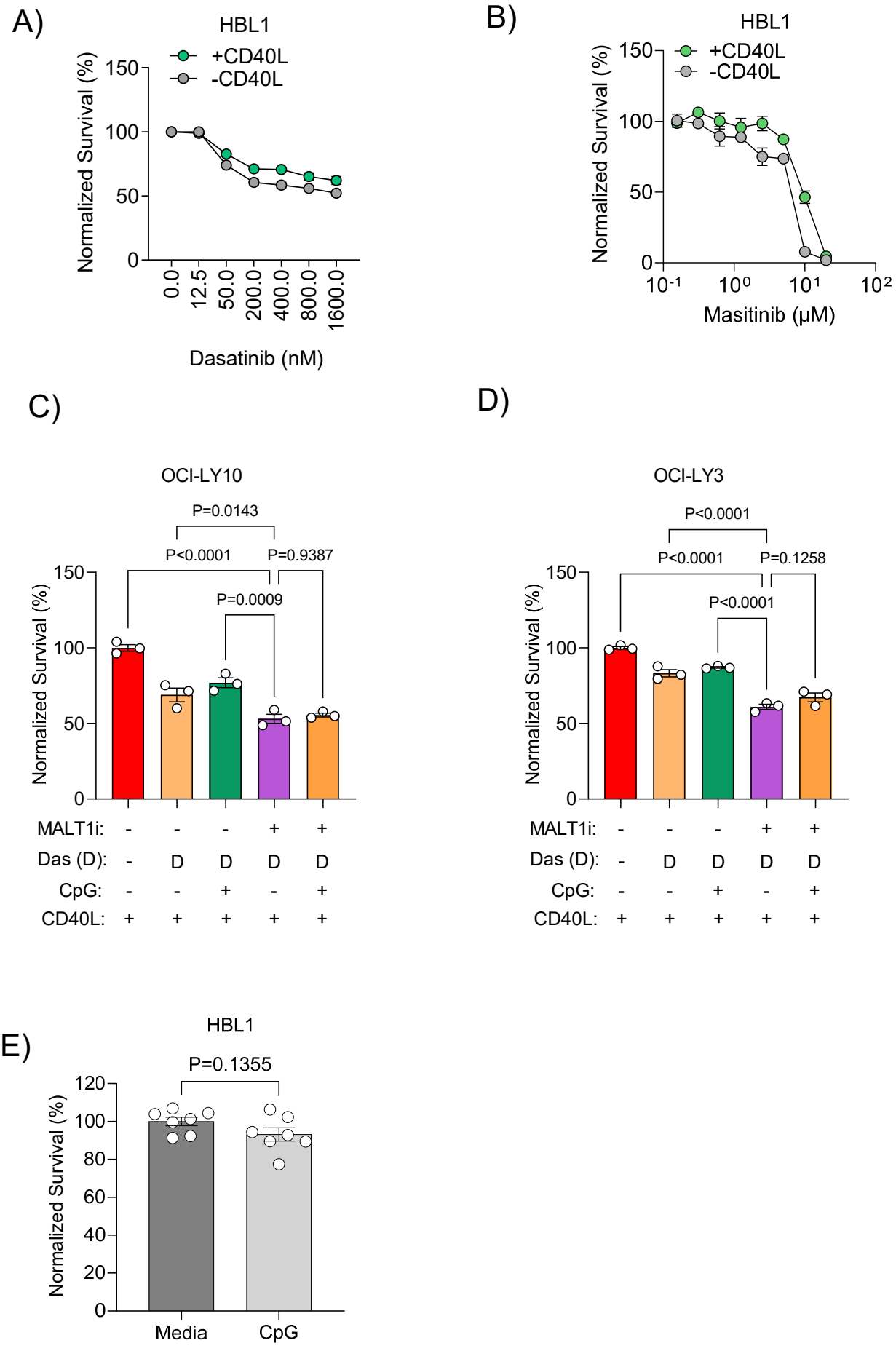

Supplementary Figure 10. Characterization of tumor cell survival under MALT1 amplifying conditions.

A-B) Survival (normalized to vehicle-treated) of HBL1 cells cultured with or without CD40L after 48 hours of culture and subsequent 48-hour treatment with increasing concentration of SRC inhibitors – dasatinib (A) or masitinib (B). Each dot represents mean ± SEM of 3 hydrogel-based organoids. C-D) Survival (normalized to vehicle-treated) of OCI-LY10 cells (C) and OCI-LY3 cells (D) cultured with CD40L-stromal cells for 96 hours, during which organoids were treated for 96 hours with 1 μM CpG and 48 hours with 2000 nM MI2, 1600 nM dasatinib. One-way ANOVA with Dunnett's multiple-comparison test was conducted in reference to groups highlighted in purple -MI2/dasatinib (mean ± SEM, n=3, where each dot is a hydrogel-based organoid). E) Survival (normalized to vehicle-treated) of HBL1 cells after 48 hours of culture in REDV-functionalized organoids without and with CpG. Two-tailed unpaired t-test (mean ± SEM, n=7, where each dot is a hydrogel-based organoid).

Supplementary Figure 11

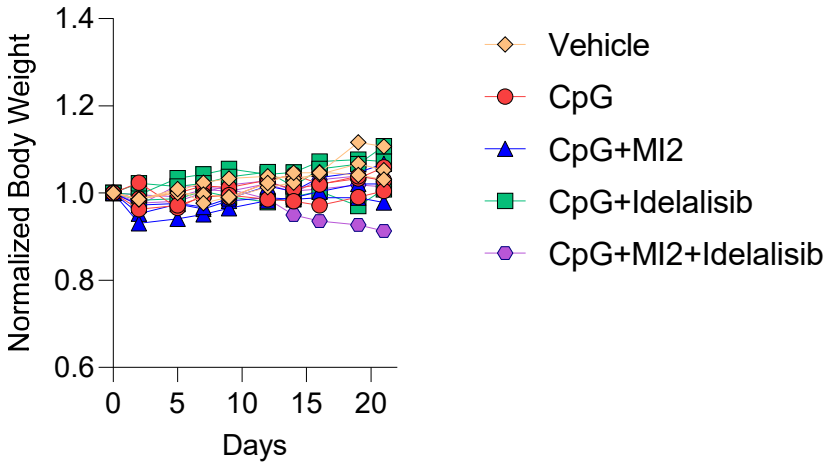

Supplementary Figure 11. Percent change in normalized body weight of NSG mice for indicated treatment groups.
Mice were treated daily with 1 mg/kg CpG intratumorally as well as 25 mg/kg MI2 and/or 40 mg/kg idelalisib intraperitoneally. Results indicate the mean ± SEM of 3 replicates.

Supplementary Figure 12

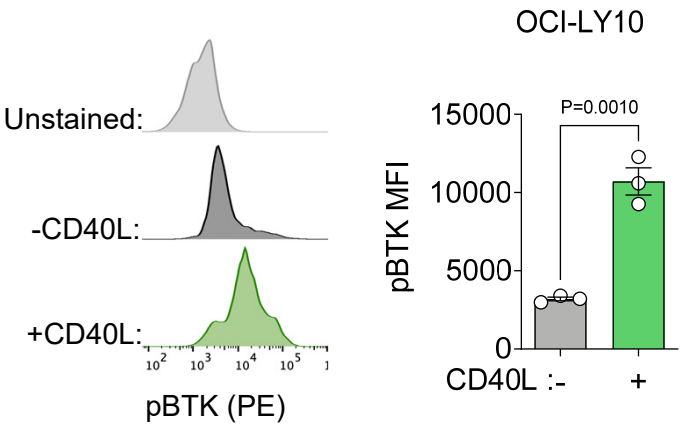

Supplementary Figure 12. Expression of pBTK after culture with CD40L expressing stromal cells.

Left: Representative flow cytometry histograms.Right: pBTK median fluorescent intensity in human ABC-DLBCL cells cultured in organoids with and without CD40L-stromal cells for 96 hours. Two-tailed unpaired t-test (mean ± SEM, n=3, where each dot is a hydrogel-based organoids).

Supplementary Table 1. GSEA comparing HBL1 cells cultured in REDV-functionalized hydrogels with and without CD40L cells.

Supplementary Table 2. GSEA comparing HBL1 cells cultured in REDV versus GFOGER-functionalized hydrogels without CD40L cells.

Supplementary References

1. LeBlanc, A.K. et al. Perspectives from man's best friend: National Academy of Medicine's Workshop on Comparative Oncology. *Sci Transl Med* **8**, 324ps325 (2016).
2. Elvers, I. et al. Exome sequencing of lymphomas from three dog breeds reveals somatic mutation patterns reflecting genetic background. *Genome Res* **25**, 1634-1645 (2015).
3. Villarnovo, D., McCleary-Wheeler, A.L. & Richards, K.L. Barking up the right tree: advancing our understanding and treatment of lymphoma with a spontaneous canine model. *Curr Opin Hematol* **24**, 359-366 (2017).
4. Richards, K.L. et al. Gene profiling of canine B-cell lymphoma reveals germinal center and postgerminal center subtypes with different survival times, modeling human DLBCL. *Cancer Res* **73**, 5029-5039 (2013).